$NH_2CH(CH_2SO_3)COO)]^+$ and $[Co(en)_2((S)\text{-}NH_2CH(CH_2SO_3)\text{-}COO)]^+$.

The experiments were again repeated, this time in 1 M NaN_3 containing NaOH (0.5 M). On mild-acid quenching (CH_3COOH) and chromatography using $NaClO_4$ eluant (1 M, pH 3), the presence of the deep purple competition product was clearly evident as a 1+ band on the column.

Controlled Chlorination of $[Co(en)_2(NH_2(CH_2)_2SO)]^{2+}$. Each of the diastereoisomers of $[Co(en)_2(NH_2(CH_2)_2SO)]^{2+}$ was treated in saturated aqueous solution with exactly 1 equiv of *N*-chlorosuccinimide, added very slowly with vigorous stirring. From the product mixture, only starting material, **10** and **11**, could be isolated—there were no significant amounts of either diastereoisomer[14] of $[Co(en)_2(NH_2(CH_2)_2SOO)]^{2+}$.

Proton NMR Spectral Studies. The ^1H NMR spectra (D_2O) of the Λ- and Δ-$[Co(en)_2((R)\text{-}NH_2CH(CO_2H)CH_2SO_2O)]^{2+}$ diastereoisomers are distinct but display the same signal pattern. The CH proton appears as a doublet of doublets, coupled to each of the inequivalent α-methylene protons, while the CH_2 protons are a complex multiplet, characteristic of the AB part of an ABX system.

The ^1H NMR spectra of the $[Co(en)_2((R)\text{-}NH_2CH(CH_2SO_3)COO)]^+$ diastereoisomers are simpler [Λ, δ 3.50 (d, J = 4 Hz, $-CH_2-$), 4.05 (t, J = 4 Hz, $-CH-$); Δ, δ 3.58 (d, J = 4 Hz, $-CH_2-$), 3.98 (t, J = 4 Hz, $-CH-$). At 60-MHz resolution, the CH proton appears as a triplet and the (diastereotopic) CH_2 protons are located at higher field as a doublet. In basic D_2O, the exchange of the CH proton of either isomer is coincident with the appearance of its epimer in the NMR spectrum. The CH triplet is depleted in time but is not replaced by a signal due to the other isomer. However, the CH_2 doublet of one isomer is replaced by the CH_2 singlet of the monodeuteriated epimer, the equilibrium distribution being 60:40 [Λ-(*R*):Λ-(*S*) or Δ-(*S*):Δ-(*R*)], starting with either form. The mutarotation is relatively rapid at pH ca. 12 in CO_3^{2-} media. Isomer assignments were confirmed by adding authentic specimens and noting intensity increases for the relevant signals.

The equilibrium isomer distribution was confirmed by chromatography of the products starting with each isomer in turn. As has been found for many other N,O-chelated amino acid complexes of this kind, Dowex 50W-X2 resin (200–400 mesh; Na^+ form) with a sodium phosphate buffer as eluant was effective in separating the diastereoisomers.

It was observed that CH exchange in the product $[Co(en)_2((R)\text{-}NH_2CH(CH_2SO_3)COO)]^+$ isomers was much faster than the rate of base hydrolysis of the parent chelated sulfonato species, $[Co(en)_2((R)\text{-}NH_2CH(CO_2)CH_2SO_2O)]^+$. Also, it seemed that the $[Co(en)_2((R)\text{-}NH_2CH(CO_2)CH_2SO_2O)]^+$ species underwent some exchange at the methine carbon, and consequently some epimerization, at a rate comparable to that for their base hydrolysis. These observations are in accord with product analyses.

Isomer Interconversions. Aside from the rearrangements described immediately above, the only other reactions to be investigated were the conversions of the two forms (Λ, Δ) of $[Co(en)_2((R)\text{-}NH_2CH(CO_2H)\text{-}CH_2SO_2O)]^{2+}$ to the corresponding forms of $[Co(en)_2((R)\text{-}NH_2CH\text{-}(CH_2SO_3)COO)]^+$. These were carried out by refluxing in 0.01 M $HClO_4$; progress was followed by chromatography on Dowex and monitoring of the two bands (the reactant and one product) by visible spectroscopy and optical rotation measurements. In this way the retention about cobalt was confirmed.

Acknowledgment. We thank the Microanalytical Service of the Australian National University for C, H, N, S, and Cl analyses.

Registry No. Λ-**1**, 62697-05-6; Δ-**1**, 62698-03-7; Λ-**4**, 112835-55-9; Δ-**4**, 112835-54-8; Λ-(*R*)-**5**·Cl, 112791-12-5; Λ-(*R*)-**5**·ClO_4, 112791-14-7; Δ-(*S*)-**5**·Cl, 112713-75-4; Δ-(*S*)-**5**·ClO_4, 112713-65-2; Δ-(*R*)-**5**·Cl, 112835-52-6; Λ-**6**·ClO_4, 112713-77-6; Λ-**6**·Cl·HCl, 112713-82-3; Λ-**6**·ClO_4·0.5$HClO_4$, 112713-79-8; Λ-**6**·Cl·0.5HCl, 112713-80-1; Λ-**6**·I·0.5HI, 112713-81-2; Δ-**6**·Cl·HCl, 112791-19-2; Δ-**6**·ClO_4·0.5$HClO_4$, 112791-18-1; Δ-**6**·HS_2O_6, 112791-16-9; **9**·2Cl, 112713-70-9; **9**·2I, 112713-71-0; **9**·2ClO_4, 112713-73-2; **9**·Cl·ClO_4, 112713-74-3; **10**·0.5S_2O_6, 112713-68-5; **10**·Cl, 76316-84-2; **10**·ClO_4, 112713-69-6; **10**·ClO_4·$HClO_4$, 112713-83-4; $[Co(en)_2(NH_2(CH_2)_2S)]^{2+}$, 42901-32-6; Λ-$[Co(en)_2((R)\text{-cys-}N,O)]^{2+}$, 112791-10-3; Δ-$[Co(en)_2((R)\text{-cys-}N,O)]^{2+}$, 112791-11-4; Λ,Δ-$[Co(en)_2((R)\text{-cys-}N,O)]_2^{4+}$, 112835-51-5; Δ,Δ-$[Co(en)_2((R)\text{-cys-}N,O)]_2^{4+}$, 64085-29-6; $[Co(en)_2(NH_2(CH_2)_2SO_2\text{-}N,S)]^{2+}$, 75249-42-2; *cis*-$[Co(en)_2Cl(NH_2(CH_2)_2SH)]^{2+}$, 112713-66-3; Λ-$[Co(en)_2((R)\text{-}NH_2\text{-}(CH_2)_2SO\text{-}N,S)]^{2+}$, 83917-58-2; Λ-$[Co(en)_2((S)\text{-}NH_2(CH_2)_2SO\text{-}N,\text{-}S)]^{2+}$, 83709-29-9; Cl_2, 7782-50-5; *N*-chlorosuccinimide, 128-09-6; *N*-bromosuccinimide, 128-08-5.

Contribution from the Department of Inorganic Chemistry, University of Sydney, Sydney, NSW 2006, Australia

Molecular Mechanics Analysis of the Influence of Interligand Interactions on Isomer Stabilities and Barriers to Isomer Interconversion in Diammine- and Bis(amine)bis(purine)platinum(II) Complexes

Trevor W. Hambley

Received September 18, 1987

A molecular mechanics analysis of the factors influencing isomer preferences and ligand rotation barriers in diammine- and bis(amine)bis(purine)platinum(II) complexes shows that the major factor is the nature of the interaction between the ammine or amine ligands and the group in the 6-position of the purine ligands. For complexes of guanine with small ammine or amine ligands, calculated barriers are less than 30 kJ mol^{-1}, and for complexes of adenine, the barriers are greater than 40 kJ mol^{-1}. The difference arises because the oxygen group in the 6-position of guanine hydrogen bonds with an ammine ligand, but the NH_2 group in the 6-position of adenine interacts unfavorably with the ammine. Barriers for complexes of guanine and adenine with tertiary amine ligands are greater than 80 kJ mol^{-1} as a result of highly unfavorable interactions between the group in the 6-position of either guanine or adenine and the bulky amine. In all cases the calculated barriers agree with experimentally determined values. In general, the head-to-tail isomer is more stable than the head-to-head isomer. For $[Pt(NH_3)_2(9\text{-ethylguanine})_2]^{2+}$, which isomer is preferred is determined by the number of intramolecular hydrogen bonds that are assumed to form.

Introduction

The primary interaction between the anticancer drug cisplatin [*cis*-diamminedichloroplatinum(II)] and its putative intracellular target, DNA, is a bifunctional attachment to adjacent guanine residues on one strand.[1] A similar, but less frequent, attachment to adjacent adenine and guanine residues has also been reported.[2] As a consequence, there has been considerable interest[3–16] in

Chart I

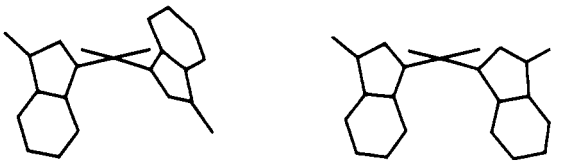

HTT HTH

diammine- and bis(amine)bis(purine)platinum(II) (*cis*-$[PtA_2Pu_2]^{x+}$, where A_2 represents two monodentate ammine or

(1) Pinto, A. L.; Lippard, S. J. *Biochim. Biophys. Acta* **1985**, *780*, 167–80.
(2) Fichtinger-Schepman, A. M. J.; van der Veer, J. L.; den Hartog, J. H. J.; Lohman, P. H. M.; Reedijk, J. *Biochemistry* **1985**, *24*, 707–13.

0020-1669/88/1327-1073$01.50/0

amine ligands or one bidentate amine ligand and Pu represents a purine base, purine nucleotide, or purine nucleotide phosphate) complexes as the simplest models for these interactions.

NMR studies of a number of *cis*-$[PtA_2Pu_2]^{x+}$ complexes have revealed a wide range of barriers to rotation about the Pt–N(7) bond.[3-5,12-16] In a bis(purine) complex, rotation about this bond results in interconversion of the head-to-head (HTH) isomer to the head-to-tail (HTT) isomer (Chart I). In complexes of 6-oxopurines with small amine ligands [e.g. $(NH_3)_2$, 1,2-ethanediamine (en), 1,3-propanediamine (tn)], it is found that this rotation and interconversion is very rapid, faster than the NMR experiment can delineate.[15,16] When the amine ligands are replaced by bulkier ligands [e.g. *N,N,N',N'*-tetramethyl-1,2-ethanediamine (tmen), *N,N,N',N'*-tetramethyl-1,3-propanediamine (tmtn)], interconversion becomes slow, and inversion barriers have been estimated by analysis of variable-temperature NMR spectra.[4,15] In contrast, complexes of 6-aminopurine species such as adenine show slow rotation with even small amine ligands, and it has been suggested that this is a consequence of the larger steric bulk of the NH_2 group in the 6-position compared with that of the oxygen atom.[14]

In the majority of cases the NMR spectra of *cis*-$[PtA_2Pu_2]^{x+}$ complexes have been interpreted in terms of a preference for the HTT isomer, and it has been suggested that this is due to fewer unfavorable steric interactions between the six-membered rings of the purine in this isomer than in the HTH isomer.[14] Most crystal structures of *cis*-$[PtA_2Pu_2]^{x+}$ species have revealed the HTT isomer,[5-9] which accords with the NMR observations. However, the structures of the cation $[Pt(NH_3)_2(9\text{-EtGua})_2]^{2+}$ (9-EtGua = 9-ethylguanine) with four different counteranions revealed in every case the HTH isomer.[10,11] The HTH isomer is, of course, a better model for the bifunctional binding of cisplatin to a single DNA strand, and it is of interest to establish the factors that determine the preference for one isomer over the other. Also, it has been suggested that one of the reasons for cisplatin binding preferentially to guanine residues over adenine residues might be steric interactions between the drug and adenine and consequent restricted rotation about the Pt–N(7) bond in the initially formed monofunctional adduct.[14] Thus, it may be that interactions which restrict rotation may influence binding to DNA, and it is therefore of interest to also determine the factors that contribute to restricted rotation in these models for the bifunctional binding of cisplatin.

We have undertaken an analysis of the steric factors influencing isomeric preferences and barriers to isomer interconversion for a range of *cis*-$[PtA_2Pu_2]^{x+}$ complexes by molecular mechanics and report the results herein. This analysis, in addition to providing information on steric influences on isomer preferences, is expected to be a good test for the molecular mechanics force field that is in use in modeling cisplatin interactions with duplex polynucleotide fragments.[17,18]

Table I. Force Field Parameters

(i) Bond Length Deformation, $E_b = {}^1/_2k_r(r - r_0)^2$

	r_0/Å	k_r/kJ mol^{-1} Å^{-2}
Pt–N(amine)	2.030	1531
Pt–N(purine)	2.010	1531

(ii) Valence Angle Deformation, $E_\theta = {}^1/_2k_\theta(\theta - \theta_0)^2$

	θ_0/deg	k_θ/kJ mol^{-1} rad^{-2}
Pt–N(7)–C(8)	127.3	181
Pt–N(7)–C(5)	127.3	181
C(5)–C(4)–C(9)	106.2	584
C(4)–C(5)–N(7)	109.5	584
C(5)–N(7)–C(8)	105.5	584
N(7)–C(8)–N(9)	112.3	584
C(4)–N(9)–C(8)	106.5	584

(iii) Out-of-Plane Deformation, $E_\delta = {}^1/_2k_\delta\delta^2$

	k_δ/kJ mol^{-1}
Pt	602

Table II. Minimized Strain Energies (kJ mol^{-1})

	isomer		
complex	HTH	HTT	HTH–HTT
$[Pt(NH_3)_2(9\text{-EtGua})_2]^{2+}$			
0 H bonds	15.4	17.4	−2.0
1 H bond	1.7	5.0	−3.3
2 H bonds	−17.0	−23.2	6.2
$[Pt(NH_3)_2(Guo)_2]^{2+}$			
0 H bonds	18.6	14.8	3.8
2 H bonds	11.2	−6.1	17.3
$[Pt(tmen)(9\text{-EtGua})_2]^{2+}$	41.1	36.9	4.2
$[Pt(NH_3)_2(9\text{-EtAde})_2]^{2+}$	6.3	3.8	2.5
$[Pt(en)(9\text{-EtAde})_2]^{2+}$	22.2	18.7	3.5
$[Pt(NH_3)_2(Ado)_2]^{2+}$	43.7	27.3	16.4
$[Pt(en)(Ado)_2]^{2+}$	57.8	44.3	13.5

Experimental Section

The Model. Strain energies were calculated according to the formalism

$$E_{tot} = \sum E_b + \sum E_\theta + \sum E_\varphi + \sum E_\sigma + \sum E_{nb} + \sum E_{hb} + \sum E_\epsilon$$

where E_b represents bond deformation energy, E_θ valence angle deformation energy, E_φ torsion angle deformation energy, E_σ out-of-plane deformation energy, E_{nb} nonbonded interaction energy, E_{hb} hydrogen-bond energy, and E_ϵ electrostatic interaction energy. Force field parameters for the metal-centered interactions were based on principles outlined by us previously.[19] In particular, 1,3-nonbonded interactions between ligating atoms were included in the model and M–N–X angle deformation constants were assumed to be independent of the particular metal and were therefore taken from previously established values for Co(III) complexes. Force constants for the purine moieties were taken initally from the all-atom force field for nucleotides reported by Weiner et al.[20] Small changes in bond angles of the five-membered ring of the purine bases were necessary to reproduce the effects of metal binding. The Pt–N(7) bond was treated in the same way as the Pt–N(amine) bonds, and Pt–N(7)–C angles were assigned force constants 50% higher than those for Pt–N(amine)–C and C–N(amine)–C angles. Values for undeformed bond lengths and angles were adjusted to give best fit to reported crystal structures and then tested by their ability to reproduce the bond lengths in other structurally characterized complexes.

Modeling hydrogen-bonding interactions between the amine ligands and the purine presents a greater problem since neither charges on the H(amine) atoms nor parameters for hydrogen bonds involving these atoms are known. Charges on atoms are generally taken from quantum-mechanical calculations, but these are still not feasible for most metal complexes. Crystal structure analyses reveal N(ammine)–O(6) distances of 2.91–2.97 Å, indicating relatively weak hydrogen bonds,

(3) Cramer, R. E.; Dahlstrom, P. L. *J. Clin. Hermatol. Oncol.* **1977**, *7*, 330–7.
(4) Cramer, R. E.; Dahlstrom, P. L. *J. Am. Chem. Soc.* **1979**, *101*, 3679–81.
(5) Cramer, R. E.; Dahlstrom, P. L. Seu, M. J. T.; Norton, T.; Kashiwagi, M. *Inorg. Chem.* **1980**, *19*, 148–54.
(6) Gellert, R. W.; Bau, R. *J. Am. Chem. Soc.* **1975**, *97*, 7379–80.
(7) Kistenmacher, T. J.; Chiang, C. C.; Chalilpoyil, P.; Marzilli, L. G. *J. Am. Chem. Soc.* **1979**, *101*, 1143–8.
(8) Marzilli, L. G.; Chalilpoyil, P. Chiang, C. C.; Kistenmacher, T. J. *J. Am. Chem. Soc.* **1980**, *102*, 2480–2.
(9) Kistenmacher, T. J.; Chiang, C. C.; Chalilpoyil, P.; Marzilli, L. G. *Biochem. Biophys. Res. Commun.* **1978**, *84*, 70–5.
(10) Lippert, B.; Raudaschl, G.; Lock, C. J. L.; Pilon, P. *Inorg. Chim. Acta* **1984**, *93*, 43–50.
(11) Schollorn, H.; Randaschl-Sieber, G.; Muller, G.; Thewalt, U.; Lippert, B. *J. Am. Chem. Soc.* **1985**, *107*, 5932–7.
(12) Gullotti, M.; Pachioni, G.; Pasini, A.; Ugo, R. *Inorg. Chem.* **1982**, *21*, 2006–14.
(13) Cramer, R. E.; Dahlstrom, P. L. *Inorg. Chem.* **1985**, *24*, 3420–4.
(14) Reily, M. D.; Marzilli, L. G. *J. Am. Chem. Soc.* **1986**, *108*, 6785–93.
(15) Marcelis, A. T. M.; van der Veer, J. L.; Zwelsoot, J. C. M.; Reedijk, J. *Inorg. Chim. Acta* **1983**, *78*, 195–203.
(16) Dijt, F. J.; Canters, G. W.; den Hartog, J. H. J.; Marcelis, A. T. M.; Reedijk, J. *J. Am. Chem. Soc.* **1984**, *106*, 3644–7.
(17) Hambley, T. W. *Inorg. Chim. Acta* **1987**, *137*, 15–7.
(18) Hambley, T. W. *J. Chem. Soc., Chem. Commun.*, in press.
(19) Hambley, T. W.; Hawkins, C. J.; Palmer, J. A.; Snow, M. R. *Aust. J. Chem.* **1981**, *34*, 45–56.
(20) Weiner, S. J.; Kollman, P. A.; Nguyen, D. T.; Case, D. A. *J. Comput. Chem.* **1986**, *7*, 230–52.

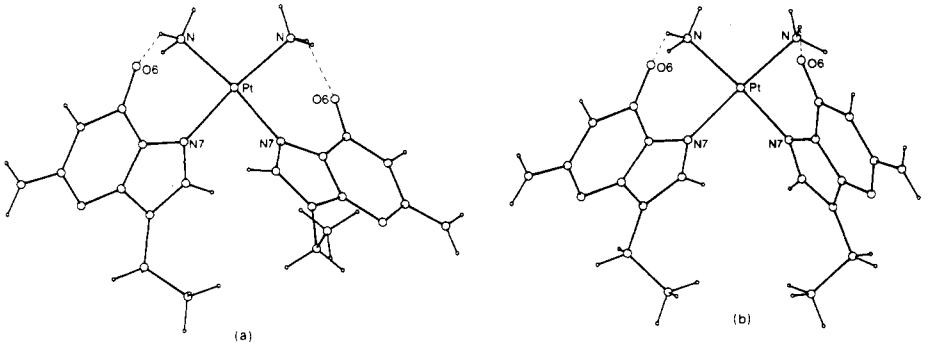

Figure 1. HTT (a) and HTH (b) isomers of $[Pt(NH_3)_2(9\text{-EtGua})_2]^{2+}$. The dashed lines indicate hydrogen bonds.

similar to those found between base pairs in DNA. On the basis of this analogy, a function of the form

$$E_{hb} = Cr^{-12} - Dr^{-10}$$

with parameters and charges used to model the interstrand hydrogen bonding of DNA in the AMBER force field[20] were used. This model was successful in reproducing the N···O hydrogen-bonding distance observed in the crystal structure of $[Pt(NH_3)_2(9\text{-EtGua})_2][Pt(CN)_4]\cdot 3H_2O$.[11]

The force field parameters not taken directly from earlier force fields for metal complexes or from AMBER are listed in Table I.

Energy Minimization. Strain energies were minimized by the full-matrix Newton–Raphson method of Boyd,[21] by using a program developed in these laboratories.[22] Minimization was continued until all shifts in positional coordinates were less than 0.001 Å. Barriers to isomer interconversion were estimated by driving one N(amine)–Pt–N(7)–C(8) torsion angle from the value for one isomer to that for the other. The torsion angle was constrained at 10° intervals in this range by the method of Langrangian multipliers[23] and the strain energy minimized in the reduced space.

Results and Discussion

$[Pt(NH_3)_2(9\text{-EtGua})_2]^{2+}$. Strain energies for all complexes considered are listed in Table II. Intramolecular hydrogen bonds between H(amine) atoms and O(6) atoms have been observed in a number of $[Pt(NH_3)_2(Pu)_2]^{2+}$ complexes, and therefore strain energies were determined for models with zero, one, or two such hydrogen bonds explicitly included. The results obtained show a dependence on the number of hydrogen bonds included. Calculations for the zero-hydrogen-bond model shows a small preference for the HTH isomer over the HTT, and this preference is increased to 3.3 kJ mol^{-1} in the one-hydrogen-bond model but is reversed to a 6.2 kJ mol^{-1} preference for the HTT isomer in the two-hydrogen-bond model. There are no very strong interactions between the purine ligands, though, as expected, they are greater in the HTH isomer, and this is reflected in a more open N(7)–Pt–N(7) angle of 88.0° compared with the 83.2° in the HTT isomer. Interactions between the purines are greater in models with hydrogen bonds included since they result in more constrained orientations of the purines. The preference for the HTT isomer in the two-hydrogen-bond model is due almost entirely to stronger hydrogen bonding in that isomer. Thus, the isomer that is expected to predominate depends on how many of the hyrogen bonds form. If the stabilizing contribution of the hydrogen bonds is subtracted from the total energy, then it is seen that formation of the hydrogen bonds results in an increase in the "strain" energy of about 2.5 kJ mol^{-1} for the first hydrogen bond and about 6 kJ mol^{-1} for the second. This increased strain would easily be accounted for by the gain in energy from hydrogen-bond formation, and therefore both such bonds would be expected to form in an isolated environment. However, in a solid-state environment, both the amine ligand and the O(6) atom are able to form stable hydrogen bonds to other complexes, solvent molecules, or anions, and then the increase in internal strain would mitigate against the formation of the intramolecular hydrogen bonds. The crystal structures of a number of salts $[Pt(NH_3)_2(9\text{-EtGua})_2]^{2+}$ reveal one intramolecular hydrogen bond and a HTH arrangement of the purine groups. Evidently the preference for the formation of intramolecular hydrogen bonds overcomes the small amount of strain that results from the formation of one such bond but not the larger amount resulting from two. The observed HTH arrangement is the isomer of minimum energy for a one-hydrogen-bond model. It should be noted that in solution formation

Table III. Comparison of Crystal Structure and Energy-Minimized Geometries for *cis*-$[Pt(NH_3)_2(9\text{-EtGua})_2]^{2+}$

atoms	cryst struct	mol mech
Pt–N(10)	2.046 (7)	2.037
Pt–N(11)	2.044 (6)	2.037
Pt–N(71)	2.022 (7)	2.022
Pt–N(72)	2.002 (6)	2.020
N(10)–Pt–N(11)	87.8 (3)	94.9
N(10)–Pt–N(72)	91.8 (3)	91.3
N(11)–Pt–N(71)	91.3 (3)	91.3
N(71)–Pt–N(72)	89.2 (3)	82.3
Pt–N(7)–C(5)	128.8 (5)	127.7
	128.2 (5)	127.6
Pt–N(7)–C(8)	124.6 (6)	126.6
	126.0 (6)	126.3
C(6)–N(1)–C(2)	123.8 (7)	124.9
	123.4 (7)	124.8
N(2)–C(2)–N(1)	114.2 (7)	118.1
	115.8 (7)	118.1
N(2)–C(2)–N(3)	122.9 (8)	119.3
	119.9 (7)	119.3
N(1)–C(2)–N(3)	122.8 (8)	122.5
	124.2 (7)	122.5
C(2)–N(3)–C(4)	114.3 (7)	113.3
	112.6 (7)	113.3
N(9)–C(4)–N(3)	126.9 (7)	126.2
	124.8 (7)	126.1
N(9)–C(4)–C(5)	105.5 (7)	106.3
	107.6 (7)	106.4
N(3)–C(4)–C(5)	127.6 (7)	127.4
	127.6 (8)	127.4
N(7)–C(5)–C(4)	108.6 (7)	109.6
	108.9 (7)	109.6
N(7)–C(5)–C(6)	133.7 (7)	130.3
	131.0 (7)	130.3
C(4)–C(5)–C(6)	117.7 (7)	120.9
	119.6 (7)	119.9
O(6)–C(6)–C(5)	127.9 (7)	127.7
	129.2 (7)	127.8
O(6)–C(6)–N(1)	119.4 (7)	120.4
	119.0 (7)	120.4
C(5)–C(6)–N(1)	113.6 (7)	111.9
	111.8 (7)	111.8
N(7)–C(8)–N(9)	110.2 (7)	112.6
	112.0 (8)	112.7
C(9)–N(9)–C(8)	127.2 (7)	127.7
	126.1 (8)	128.0
C(9)–N(9)–C(4)	123.7 (7)	126.0
	127.3 (7)	125.8
C(8)–N(9)–C(4)	109.1 (7)	105.9
	105.9 (7)	105.9
C(9′)–C(9)–N(9)	113.1 (8)	109.9
	107.4 (9)	110.4

(21) Boyd, R. H. *J. Chem. Phys.* **1968**, *49*, 2574–83.
(22) Hambley, T. W. "MOMEC-87, A Program for Strain Energy Minimization"; University of Sydney, 1987.
(23) Hambley, T. W. *J. Comput. Chem.* **1987**, *8*, 651–7.

Table IV. Angles (deg) between Planes through the Two Purine Ligands (1) and between Each of the Purine Ligands and the Coordination Plane (2, 3)

	HTH			HTT		
complex	1	2	3	1	2	3
$[Pt(NH_3)_2(9\text{-EtGua})_2]^{2+}$						
0 H bonds	89.9	92.0	73.8	76.8	91.6	93.6
1 H bond	75.1	60.7	54.5	47.6	76.0	65.9
2 H bonds	83.4	66.0	66.0	42.9	54.0	66.1
$[Pt(NH_3)_2(Guo)_2]^{2+}$						
0 H bonds	56.7	64.8	58.3	57.0	97.0	96.9
2 H bonds	83.9	65.8	61.6	59.0	63.4	68.2
$[Pt(tmen)(9\text{-EtGua})_2]^{2+}$	75.7	93.1	86.3	81.2	96.2	96.6
$[Pt(NH_3)_2(9\text{-EtAde})_2]^{2+}$	86.0	75.8	79.5	73.5	86.6	92.4
$[Pt(en)(9\text{-EtAde})_2]^{2+}$	87.2	80.3	82.0	73.2	86.1	92.7
$[Pt(NH_3)_2(Ado)_2]^{2+}$	67.9	72.0	58.7	61.1	98.0	97.3
$[Pt(en)(Ado)_2]^{2+}$	68.3	73.3	60.2	61.9	83.3	83.7

Table V. Calculated Barriers to Rotation about the Pt–N(7) Bond (kJ mol^{-1})

complex	energy
$[Pt(NH_3)_2(9\text{-EtGua})_2]^{2+}$	
0 H bonds	35.9
2 H bonds	22.4
$[Pt(NH_3)_2(Guo)_2]^{2+}$	
2 H bonds	27.5
$[Pt(tmen)(9\text{-EtGua})_2]^{2+}$	84.2
$[Pt(NH_3)_2(9\text{-EtAde})_2]^{2+}$	39.6
$[Pt(en)(9\text{-EtAde})_2]^{2+}$	43.4
$[Pt(NH_3)_2(Ado)_2]^{2+}$	47.7
$[Pt(en)(Ado)_2]^{2+}$	49.6

of intermolecular hydrogen bonds will not be as facile; therefore a higher population of the two-hydrogen-bond structure, and therefore, the HTT arrangement, would be expected.

The energy-minimized structure of $[Pt(NH_3)_2(9\text{-EtGua})_2]^{2+}$ with one intramolecular hydrogen bond is compared with the crystal structure of $[Pt(NH_3)_2(9\text{-EtGua})_2][Pt(CN_4)]\cdot 3H_2O$ in Table III, and angles between the planes of the purines ligands and between each of these planes and the coordination plane are given in Table IV. Views of the HTH and HTT isomers with two hydrogen bonds are shown in Figure 1.

Barriers to interconversion from HTH to HTT isomers by rotation of one ligand about the Pt–N(7) bond were estimated for models with zero and two hydrogen bonds. Barriers to rotation are collected in Table V. The zero-hydrogen-bond model is expected to be unrealistic since during the isomeric interconversion the O(6) atom of the rotated ligand must pass very close to an ammine ligand. A plot of the strain energy as a function of φ, the angle between the coordination plane and the plane through the rotated ligand for the two-hydrogen-bond model, is shown in Figure 2. The barriers obtained were 35.9 and 22.4 kJ mol^{-1} for the zero- and two-hydrogen-bond models, respectively. The former value would indicate slow rotation about the Pt–N(7) bond, and the latter, fast rotation. NMR studies of $[Pt(NH_3)_2(Pu)_2]^{2+}$ indicate fast rotation,[4,15,16] consistent with the more realistic two-hydrogen-bond model. The higher barrier in the zero-hydrogen-bond model arises because in that case the O(6)–H(amine) interactions become highly repulsive when the ligand and coordination planes are coplanar, but in the two-hydrogen-bond model they remain favorable at all times.

$[Pt(NH_3)_2(Guo)_2]^{2+}$. Models with zero, one, and two hydrogen bonds were also considered for the complex of the guanosine ligand (Guo). The results are similar to those obtained for the 9-ethylguanine ligand in that the stability of the HTT isomers decrease with the number of hydrogen bonds, but in all cases the HTT isomer is more stable than the HTH. This is a consequence of increased interligand interactions between the bulkier guanosine ligands and is reflected in a large (14.6 kJ mol^{-1}) difference in the nonbonded contributions to the strain energies of the HTH and HTT isomers.

The estimated barriers to isomer interconversion are also similar to those obtained for the 9-ethylguanine complexes but are slightly

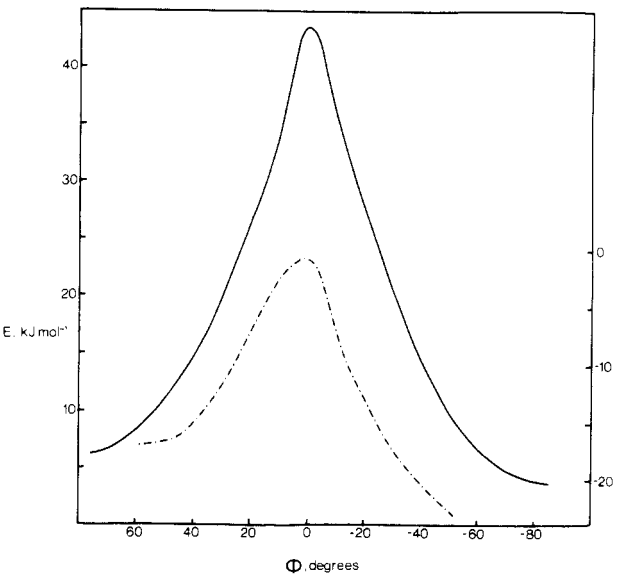

Figure 2. Strain energy plotted against the angle (φ) between the rotated purine and the coordination plane for $[Pt(NH_3)_2(9\text{-EtGua})_2]^{2+}$ (–·–, right-hand-side energy scale) and $[Pt(NH_3)_2(9\text{-EtAde})_2]^{2+}$ (—, left-hand-side energy scale).

larger in each case. The barrier for the two-hydrogen-bond model, 27.5 kJ mol^{-1}, is again consistent with rapid isomer interconversion on the NMR time scale.[4,15,16]

$[Pt(tmen)(9\text{-EtGua})_2]^{2+}$. When all amine hydrogen atoms are replaced by alkyl groups, there is of course no longer any possibility of hydrogen bonding between the guanine and the amine ligands. This has an effect on isomer preferences, equilibrium geometries, and barriers to isomer interconversions. In the case of the tmen ligand the HTT isomer is 4.2 kJ mol^{-1} more stable than the HTH. The purines lie almost perpendicular to the coordination plane (94.5 and 95.8° for HTT and 87.5 and 93.6° for HTH), and the N(7)–Pt–N(7) angle is significantly closed (by 5–10°, Figure 3). The dominant influences on the structure are the unfavorable interactions between the methyl groups of the amine ligand and the purine ligands [HTH O(6)···H(amine) = 2.62 Å, HTT O(6)···H(amine) = 2.81 Å]. These result in the purine ligands being forced closer together and so in further destabilization of the HTH isomer.

The barrier to isomer interconversion is increased dramatically over the complexes with ammine and smaller amine ligands to 84.2 kJ mol^{-1}. This agrees well with the estimate of Cramer and Dahlstrom that the barrier to isomer interconversion is about 86 kJ mol^{-1} [4] and supports their suggestion that it should be possible to separate the HTT and HTH isomers. The increased barrier results from the need to drag the O(6) atom of the purine past the methyl (amine) groups resulting in highly unfavorable interactions.

$[Pt(NH_3)_2(9\text{-EtAde})_2]^{2+}$ and $[Pt(en)(9\text{-EtAde})_2]^{2+}$ (9-EtAde = 9-Ethyladenine). On going from guanine- to adenine-based purine bases, one sees that the O(6) atom is replaced by a NH_2 group. Thus, hydrogen bonding between the purine ligand and the ammine or amine ligands is no longer possible. Consequently, the structural and isomeric properties of the complexes with adenine ligands are more similar to those of guanine complexes with tertiary amine ligands. For $[Pt(NH_3)_2(9\text{-EtAde})_2]^{2+}$ the HTT isomer is more stable than the HTH primarily because interactions between the $-NH_2$ groups of the purine and the amine ligands force the purines closer together (N(7)–Pt–N(7): HTH, 84.9°; HTT, 79.5°), and this is more easily accommodated by the HTT isomer than the HTH.

The strain energy of $[Pt(NH_3)_2(9\text{-EtAde})_2]^{2+}$ is plotted against the angle between the rotated purine and the coordination plane in Figure 2. The barrier to rotation about the Pt–N(7) bond is much larger than the barrier for the analogous guanine complex because the $-NH_2$ group of the purine must be moved past the ammine ligand, resulting in highly unfavorable interactions. The

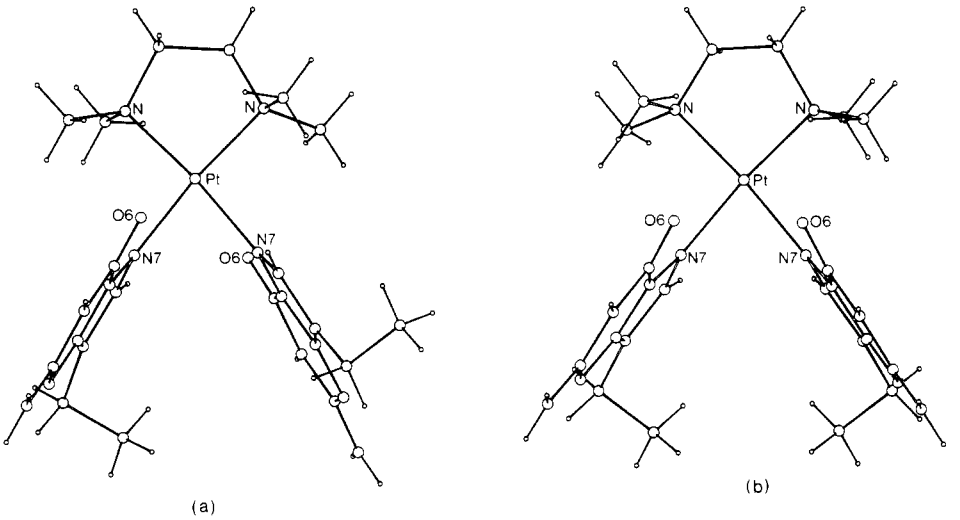

Figure 3. HTT (a) and HTH (b) isomers of $[Pt(tmen)(9\text{-}EtGua)_2]^{2+}$.

barrier is 39.6 kJ mol^{-1}, which is consistent with slow rotation on the NMR time scale.

The energy difference between the HTH and HTT isomers and the barrier to isomeric interconversion are both slightly higher for the ethylenediamine complex because of the greater inflexibility of the en ligand compared to that of the ammine ligands.

$[Pt(NH_3)_2(Ado)_2]^{2+}$ and $[Pt(en)(Ado)_2]^{2+}$ (Ado = Adenosine). The greater bulk of the adenosine ligand compared with that of 9-ethyladenine results is a significant destabilization of HTH isomer in which the purines are forced close together. This destabilization for the complex means that the HTH isomer is 13.5 kJ mol^{-1} less stable than the HTT, and therefore in solution only the latter would exist in significant quantities. The NMR spectrum of $[Pt(en)(5'\text{-}dAMP)_2]$ was interpreted as showing evidence for only the HTT isomers,[14] which accords with the calculations.

The barrier to rotation about the Pt–N(7) bond is also increased by the bulk of the adenosine ligand. For the en complex this barrier is 49.6 kJ mol^{-1}. Line shape analysis of the NMR spectrum of $[Pt(en)(5'\text{-}dAMP)_2]$ indicated a barrier of 63 ± 4 kJ mol^{-1},[14] in satisfactory agreement with the calculations. A slightly increased barrier would be expected on going from the adenosine to the adenosine 5′-monophosphate ligand because of the greater bulk of the latter ligand.

Conclusions

The wide range of barriers to rotation about the Pt-N(7) bond in bis(purine)platinum(II) complexes is reproduced well by the molecular mechanics calculations. In so doing, the calculations provide the following explanations, based on steric factors, for the observed differences:

(i) Differences in interactions between the purine and the amine or ammine ligands are almost entirely responsible for the range in barriers to rotation. When the interactions are favorable, such as the hydrogen bonds between an O(6) atom on a guanine and an ammine or amine hydrogen atom, the rotation is facile. But, when the interaction is unfavorable, such as between an $-NH_2$ group of an adenine and an ammine ligand, rotation is hindered. Thus, it is not the larger steric bulk of the $-NH_2$ group compared with that of the oxygen atom in the 6-position but rather the type of interaction between the purine and the other ligands that is responsible for changes in rotation barriers. Also, when all amine H atoms are replaced by alkyl groups, unfavorable interactions between the purine and the alkyl group result in much higher barriers.

(ii) Interactions between the purine ligands are of relatively minor importance in determining both isomer preferences and rotation barriers though they become progressively more important with increasing bulk of the purine.

(iii) In general, the HTT isomer is more stable than the HTH isomer as the result of fewer unfavorable contacts between the purine ligands. However, this is not the case for the $[Pt(NH_3)_2(9\text{-}EtGua)_2]^{2+}$ complexes and which isomer is expected depends on the number of hydrogen bonds between the purines and the ammine ligands.

These results, particularly point i, are of relevance to the binding of cisplatin and its congeners to DNA since they show that significant interactions between the nonlabile ligands on the platinum and the purine bases of DNA might result. It is interesting to note that there is a correlation between how favorable the interactions between the purine and the ammine or amine ligand are and the preferences of cisplatin to bind to DNA. Specifically, binding of platinum with ammine ligands to guanine is preferred, binding to adenine is less favored, and binding of platinum with tertiary amine ligands does not appear to occur at all. Thus, the present calculations on simple models appear to support the observations of more detailed modeling[17,18] that interactions between the ammine or amine ligands and DNA may be important determinants of binding ability.

Acknowledgment. A part of this work was performed while I was on leave at Emory University, Atlanta, GA, and I wish to thank Professor L. G. Marzilli for provision of facilities. I also wish to thank Professor Marzilli and Dr. M. D. Reily for helpful discussions.

Registry No. *cis*-$[Pt(NH_3)_2(9\text{-}EtGua)_2]^{2+}$, 79301-63-6; *cis*-$[Pt(NH_3)_2(Guo)_2]^{2+}$, 62661-45-4; $[Pt(tmen)(9\text{-}EtGua)_2]^{2+}$, 112712-58-0; *cis*-$[Pt(NH_3)_2(9\text{-}EtAde)_2]^{2+}$, 112712-59-1; $[Pt(en)(9\text{-}EtAde)_2]^{2+}$, 112712-60-4; *cis*-$[Pt(NH_3)_2(Ado)_2]^{2+}$, 103957-92-2; $[Pt(en)(Ado)_2]^{2+}$, 112712-61-5.